



Glacial retreat delineation using machine and deep learning: A case of a lower Himalayan region

SRIRAM VEMURI¹, DHWANILNATH GAUTAM^{1,*}  and SHAILY GANDHI²

¹*Faculty of Technology, CEPT University, Kasturbhai Lalbhai Campus, Ahmedabad 380 009, India.*

²*Center for Applied Geomatics (CAG), CEPT Research and Development Foundation (CRDF), CEPT University, Kasturbhai Lalbhai Campus, Ahmedabad 380 009, India.*

*Corresponding author. e-mail: dhwanielnath@gmail.com

MS received 20 July 2023; revised 24 November 2023; accepted 11 December 2023

Climate change can have adverse effects on various ecosystems on the globe, with the cryosphere being affected to a significant extent. Of the cryosphere, mountain or alpine glaciers are essential resources for freshwater and various ecosystem services. Glacial ablation is the process of removal of snow and ice from a glacier, which includes melting, evaporation, and erosion. The increase in temperature on the Earth due to climate changes is causing rapid glacial abrasion. The rapid global decline in alpine glaciers makes it necessary to identify the key drivers responsible for a glacial retreat to understand the eventual modifications to the surroundings and the Earth's ecosystem. This study attempts to understand the influence of different driving factors leading to glacier retreat using Machine Learning (ML) and Remote Sensing (RS) techniques. Three models have been developed to estimate the glacial retreat: Feedforward Artificial Neural Network (ANN), Recurrent Neural Network (RNN) and Long-Short Term Memory (LSTM). The RNN performed the best with an average training and validation accuracy of 0.9. The overall shift of the area estimate has been identified over 10 years. The model thus generated can lead to a better understanding of the region and can provide a baseline for policy and mitigation strategies in the future.

Keywords. Glacier; glacier retreat; artificial neural networks; recurrent neural networks; long-short term memory.

1. Introduction

Glaciers are permanent bodies of ice formed through the recrystallization of snow that show evidence of gravitational movement. Glaciers are an integral part of the cryosphere, where the water exists primordially in a frozen state. Presently, glaciers are found mostly in polar regions at high altitudes. Glaciers and ice sheets cover 11% of the Earth's surface and 50% of the Atlantic coastline is covered by floating ice shelves (Rees 2005).

Glaciers are dynamic systems that move by and under the influence of gravity, change drastically w.r.t. the surrounding climatic conditions. Thus, glaciers may be considered important indicators of climate change that reflect environmental changes (Romshoo *et al.* 2022; Guidicelli *et al.* 2023).

Climate change and global warming have severely affected the survival of various ecosystems around the Earth's surface and oceans. The planet has experienced various episodes of climate change with different periods of the Earth being much colder or

hotter than at present (Kusky 2010). The pace at which the planet is warming up, however, has become much more rapid that brings forward lasting longer-term consequences including but not limited to greenhouse gas-dominated atmosphere, drastic increase in sea levels, estimated to rise at a rate of 8–16 mm per year by 2100, 10 times more than that of the mean rise rate in the 20th century (Church *et al.* 2013). The factors contributing to the rise in sea levels include thermal expansion of ocean water as the water warms due to global warming and the melting of glaciers, ice caps and snow. Glaciers have been observed to be shrinking in Northern and Southern hemispheres, and the Arctic and Antarctic ice caps are also observing rapid shrinkage (Kusky 2010). Decreasing snow cover and retreating glaciers have had and continue to have vast consequences on regional ecosystems with significant implications for socio-economic development and ecosystem services (Singh *et al.* 2016).

Glaciers are permanent bodies of ice formed through the recrystallization of snow that show evidence of gravitational movement. Glaciers are an integral part of the cryosphere, where the low temperatures imply that the water exists primordially in a frozen state. Most glaciers presently are found in polar regions at high altitudes. Glaciers and ice sheets cover 11% of the Earth's surface; 50% of the Atlantic coastline is covered by floating ice shelves (Rees 2005; Pellikka and Rees 2009). Glaciers are dynamic systems that have moved in accordance with and under the influence of gravity and change drastically w.r.t. the surrounding climatic conditions. Thus, glaciers may be considered important indicators of climate change that reflect changes in the environment (Kusky 2010). Glaciers have been observed to be shrinking in Northern and Southern hemispheres, and the Arctic and Antarctic ice caps are also undergoing rapid shrinkage (Stokes *et al.* 2022). Decreasing snow cover and retreating glaciers have vast consequences on regional ecosystems with significant implications on socio-economic development and ecosystem services (Singh *et al.* 2016). The glacial landuse is a key part of the natural ecosystem that thrives within these regions. The implications of glacial retreat can have adverse effects on the system. Not only does it disrupt the natural water cycle, but the amount of ice available for replenishment will become a challenge as the over-glacial retreats (Carey *et al.* 2017). But this will also entail the effects on the natural flora and fauna. The declining ice can also develop sludge-infused mud, which can further lead to landslides and other

calamities. Impacting greatly on the natural human settlements as well (Garrard *et al.* 2016).

The observation of and collection of information from an object without direct physical contact is termed remote sensing, and observations are usually made from a space-borne or an airborne platform with the information carried over via electromagnetic radiation (Pellikka and Rees 2009). The potential for observations of environmental sciences has been vastly widened by the use of space-borne platforms, given the sheer quantity of information that can be obtained over areas on a large scale, especially the locations that may be difficult to tread via land or airborne means. Another important factor that space-borne platforms add is the continuity for data collection, with satellite missions being launched for information to be relayed over decades. All these factors prove especially advantageous when it comes to the observation of glaciers making it quicker to retrieve and exploit the satellite data, especially given the difficulties in the physical exploration of glacial terrains (Pellikka and Rees 2009).

The importance of glaciers as aforementioned, brings with it the need for their monitoring and measurement. This can be done via the quantification of the interrelationships that the glacial extent has with various affecting factors (Romshoo *et al.* 2022). The glacial zones of dry snow, firn, ice, and wet snow have distinctive reflectance characteristics. Albedo is the measure of this reflectance; it is the ratio of radiation reflected from a surface to the incident radiation on that surface. Precipitation is an integral factor in the formation of a glacier in connection to surface temperature. Precipitation is an integral factor in the formation of a glacier in connection to surface temperature (Yue *et al.* 2020). With the variations and undulations within the precipitations near the snow line, there is a lot of water accumulation. Liquid water is warmer than snow, firn or ice. Thus, wet snow zones, which can be detected easily using thermal remote sensing methods and surface temperature, play a role counter to that of precipitation in glaciers as the higher temperatures are what lead to glacial melt. The quantification of these parameters can assist in understanding the influence of these factors with each other and their collective (as well as individual) influence on the snow cover of glaciers (Dubey and Goyal 2020).

Artificial Intelligence (AI) and Machine Learning (ML) techniques have observed a rise in newer approaches to better quantify the various

interlinked variables and parameters (Gao 2020). AI can be defined as the science and engineering of making intelligent machines and/or computer programs, not necessarily confined to biologically observable methods (McCarthy 2007). The recent progress and changes in methods, techniques and the large-scale availability of quality datasets have vastly enhanced the applicability of AI (Gao 2020). In the process, geospatial-driven AI techniques have gained significant traction. Geospatial Artificial Intelligence or GeoAI is AI and ML techniques used to simulate future outcomes that run on geospatial technology, often drawing on computer vision, simulation tools and statistical modelling; it combines spatial science methods, data mining and high-performance computing to extract meaningful information from geospatial data and/or tools (Kamel Boulos *et al.* 2019). To that end, ML and DL have emerged as good tools for handling big data, especially those that may pertain to glacial parameters (Kadota *et al.* 1997; Kaushik *et al.* 2020). Through means of ML and DL, the shrinking boundary of the glacier may be effectively delineated, thus allowing for the forecasting of the same (Baraka *et al.* 2020; Bolibar *et al.* 2020). The large-scale prediction for the delineation over a region can be difficult using traditional methods, but with the use of ML (Machine Learning) and DL techniques within Geospatial Artificial Intelligence (GeoAI), these challenges can be handled. The shrinkage in glacial ice may be linked to a wide array of parameters, as previously discussed; modelling this shrinkage for estimation of the retreat can be demanding when considering traditional remote sensing techniques given the large temporal and spatial resolutions (Sood *et al.* 2022).

2. Glaciers and remote sensing

Given the difficulties in physical exploration due to the terrain inaccessibility of glacial terrains (Kulkarni *et al.* 2007), complex environmental conditions (Taloor *et al.* 2021) and inconsistencies in the availability of credible baseline data (Rafiq *et al.* 2019), various studies have preferred a remote sensing approach for glacial observations over the conventional methods of field-based observations. Glacial delineation for the observation of spatiotemporal changes in glaciers has been a common approach in making observations and estimations as to the changes and retreat in

glaciers (Patel *et al.* 2018; Kaushik *et al.* 2020; Tripathi *et al.* 2022) to observe the fluctuations in the glacial terminus and snout position (Bhambri *et al.* 2012; Patel *et al.* 2018), mapping and identification of clean ice glacier (Kaushik *et al.* 2020), influence on environmental parameters such as land surface temperature (Tripathi *et al.* 2022), topographical and geomorphological characteristics in the region such as elevation, slope and debris cover (Patel *et al.* 2018; Kaushik *et al.* 2020; Taloor *et al.* 2021). Quantifying the applicability of these parameters, a series of studies have observed the approach within the domain. Tripathi *et al.* (2022) has observed that shrinkage in glaciers and an increase in glacial lake area have vastly contributed to risks of Glacial Lake Outburst Floods (GLOFs) that are a result of the sudden discharge of large volumes of water from glacial lakes to flow downstream, that have repeatedly caused loss of lives and damages to infrastructure (Jain *et al.* 2012); the melting of glaciers has been contributed significantly by the gradual increase in surface temperature; concludes that global warming has had a drastic effect on the glacier shrinkage. Kaushik *et al.* (2020) notes that glaciers in lower elevations have retreated by considerable amounts, while the ones in higher elevations have stayed relatively stable. Patel *et al.* (2018) notes that the presence of debris cover in the glacial area greatly influences the melt rate of the glacier, while contrary to this observation, higher retreat has been observed in debris-free glaciers. The paper also notes that steeper-sloped glaciers are less sensitive to environmental factors and climate change than gentler-sloped glaciers. The general approach to the studies predominantly has been to use satellite imagery such as the Landsat series (Bhambri *et al.* 2012; Patel *et al.* 2018; Kaushik *et al.* 2020; Tripathi *et al.* 2022), Cartosat 1 (Bhambri *et al.* 2012), LISS III and IV (Kulkarni *et al.* 2007); Kaushik *et al.* (2020) applied a semi-automated technique for clean ice and snow mapping through various input parameters, which was merged with parallel output for debris cover mapping for a base glacial boundary, which has been used for change detection over different periods. In contrast to this approach, Taloor *et al.* (2021) delineated the glacier manually using geospatial tools which were then correlated with the manually derived LST. Other aforementioned studies have also relied on delineating glacial boundaries to estimate the retreat patterns. It may also be noted that using different imageries derived from different datasets

with varying properties might result in erroneous or difficult to resolve to map accuracies, thus making analysis difficult (Romshoo and Rashid 2010; Bhambri *et al.* 2012). Thus, several studies have approached glacial studies through a modelling aspect for quantifying the relationships between the aforementioned variables with that of glacial retreat.

Modelling of glaciers has largely involved physical models such as surface mass balance model (Kadota *et al.* 1997; Shea *et al.* 2015) and general circulation model (Hock 2005; Jury *et al.* 2020) for the monitoring of retreat in glaciers. Bolibar *et al.* (2020) has presented a unique approach that combines the physical modelling of glacier w.r.t. actualized through a feedforward ANN architecture for the simulation of annual surface mass balance by taking into consideration a vast array of parameters.

3. Study region and datasets

The area of focus or the ROI spans 2341.79 km², as depicted in figure 1. It is a dense mountainous region in Uttarakhand that surrounds alpine peaks

such as Gangotri Peak, Sri Kailas Peak; key glaciers in the ROI include Chorabari Glacier and Gangotri Glacier. Chorabari Glacial Lake is located in the basin of river Mandakini, near the pilgrimage Kedarnath (Das 2013). It is a valley glacier with a surface extent of 6.7 km². It is the source of the Mandakini River that joins the Alaknanda River near Rudraprayag (Mehta *et al.* 2014). The Glacial Lake flows north to south with its accumulation area below Bharatkund and Kedarnath peaks (Mehta *et al.* 2012). Gangotri is an alpine glacier originating between the peaks of Chaukhamba; Gangotri is the chief source of the Ganges River (Bhambri *et al.* 2012). The region holds special significance in the glacier retreat as many major rivers originate from the Himalayan region and pass through the region of interest. The region is also a key factor for hydroelectricity, with the entire region and beyond relying heavily on the same. Also, the region has a high human footfall on account of tourism and religious pilgrimages (Kumar *et al.* 2021a, b). The shifting landscapes due to ice reduction and glacier retreat can affect the local economy. Not only this, but as mentioned earlier, the ice sludge can lead to landslides, which

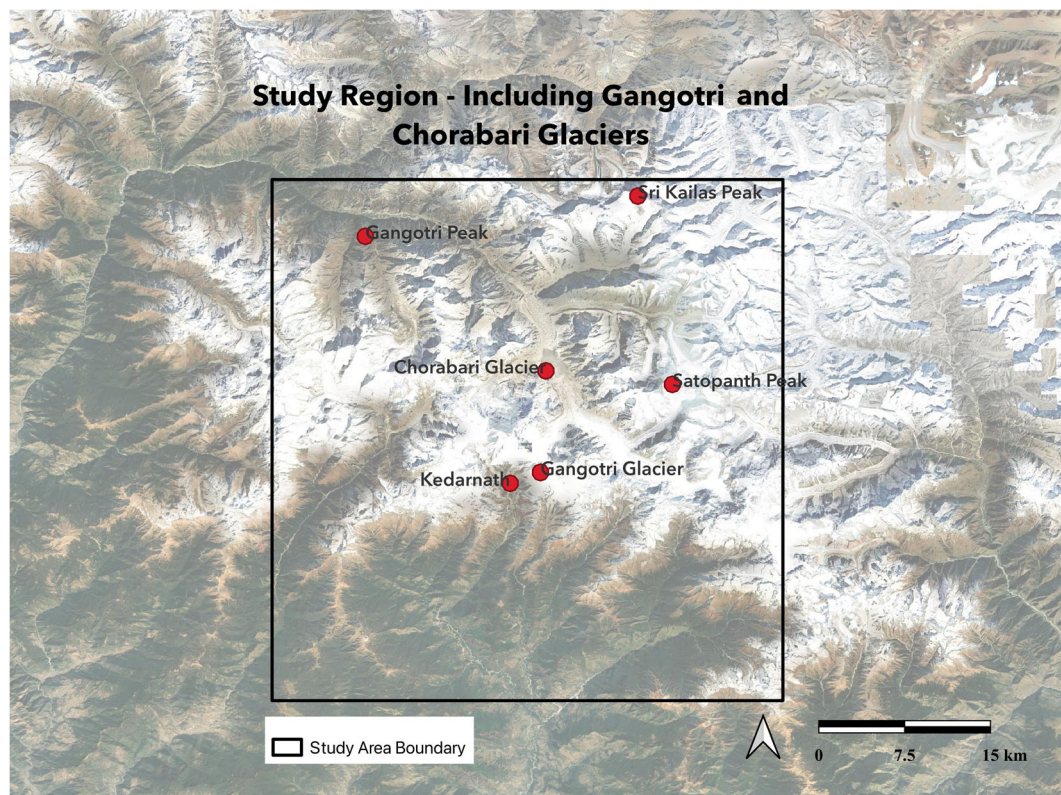


Figure 1. Area of focus.

can lead to heavy losses of life. This is also enhanced due to the phenomenon of the glacial lake outburst floods, which can result in sudden and massive floods downstream and affect communities, infrastructure, and agriculture (Khanal *et al.* 2015). The region itself plays a key role in the regional climate and its patterns have a direct influence on the southern pollution space of Delhi to the overall ice development on the north of the Upper Himalayas. The landuse change can influence the local economy as well as reduce the available natural resources, flora and fauna, which heavily rely on the cold environment (Saikawa *et al.* 2019).

The study focuses on the usage of multi-source datasets by extraction through Google Earth Engine for the sensors of MODerate Resolution Imaging Spectrometer (MODIS), Shuttle Radar Topography Mission (SRTM), European Centre for Medium-Range Weather Forecasts Reanalysis v5 (ECMWF-R) and Breathing Earth System Simulator (BESS). Datasets have been acquired from sources as mentioned in table 1. The temporal resolution of the retrieved daily datasets has been aggregated yearly, from years 2005 to 2021. Due to the temporal variations within the parameters, each parameter was scaled to match the standard references. Furthermore, the study was conducted on an yearly basis to avoid data gaps and missing observations within the study. The parameters were filtered out with cloud mask to avoid over-contamination and aggregated over an yearly basis. This pre-processing step was only undertaken for parameters without yearly observations like LST. The remaining were directly considered and scaled to match the NDSI observations. The identification of glacial delineation has been

attributed to the NDSI. A demarcation of 0.5 and higher is defined as pure snow and the boundaries have been identified through the same. The influence of different parameters needs to be understood properly. A heat map is a graphically represented correlation matrix quantifying the correlations between the different variables (Rajagopalan and Rajagopalan 2021), as depicted in figure 2 and their sources in table 1.

Given the presence of water at freezing temperatures in the surrounding area and the influence of water from precipitation in forming a glacier, as previously described, a strong correlation can be observed in NDWI with glacial ice and NDSI. Albedo is a measure of the solar energy scattered back into space upon its incidence on the Earth’s surface (Stephens *et al.* 2015); the albedo of snow, especially fresh snow surfaces, is very high (Angstrom 1925) given their higher surface reflectance, thus the strong correlations that albedo and RSDN share with glacial ice and NDSI. The glacial extent has an inverse relation with LST, as discussed in the literature review, which can be observed in the heat map. Due to the higher retreat rate of snow on higher altitudes (Ghatak *et al.* 2014), a strong inverse relation may be observed in the case of elevation with glacial ice, NDSI and albedo. Furthermore, the detailed trend patterns of 15-year aggregated and trend mean over the year have been depicted in figure 3, so as to ascertain the similarities or the dissimilarities between the parameters in the years 2005–2021.

Since the surface reflectance of snow is high, albedo would turn up higher when there is a higher incidence of snow and NDWI is following a similar trend as it is water under freezing temperatures that also contributes to the crystallization of snow

Table 1. *Parameters used within the study.*

| Datasets used in study | Symbol | Source | Resolution (m) | Source |
|-----------------------------------|--------|---------|----------------|---|
| Albedo | | MODIS | 500 | Angstrom (1925); Pellikka and Rees (2009) |
| Elevation | Z | SRTM | 30 | Jury <i>et al.</i> (2020); Sood <i>et al.</i> (2022) |
| Enhanced vegetation index | EVI | MODIS | 500 | Angstrom (1925); Baraka <i>et al.</i> (2020) |
| Land surface temperature | LST | MODIS | 1000 | Bolibar <i>et al.</i> (2020); Shea <i>et al.</i> (2015) |
| Normalised difference snow index | NDSI | MODIS | 500 | Baraka <i>et al.</i> (2020) |
| Normalised difference water index | NDWI | MODIS | 500 | Baraka <i>et al.</i> (2020) |
| Precipitation | | ECMWF-R | 11132 | Jury <i>et al.</i> (2020); Shea <i>et al.</i> (2015) |
| Shortwave radiation | RSDN | BESS | 1000 | Pellicciotti <i>et al.</i> (2005) |

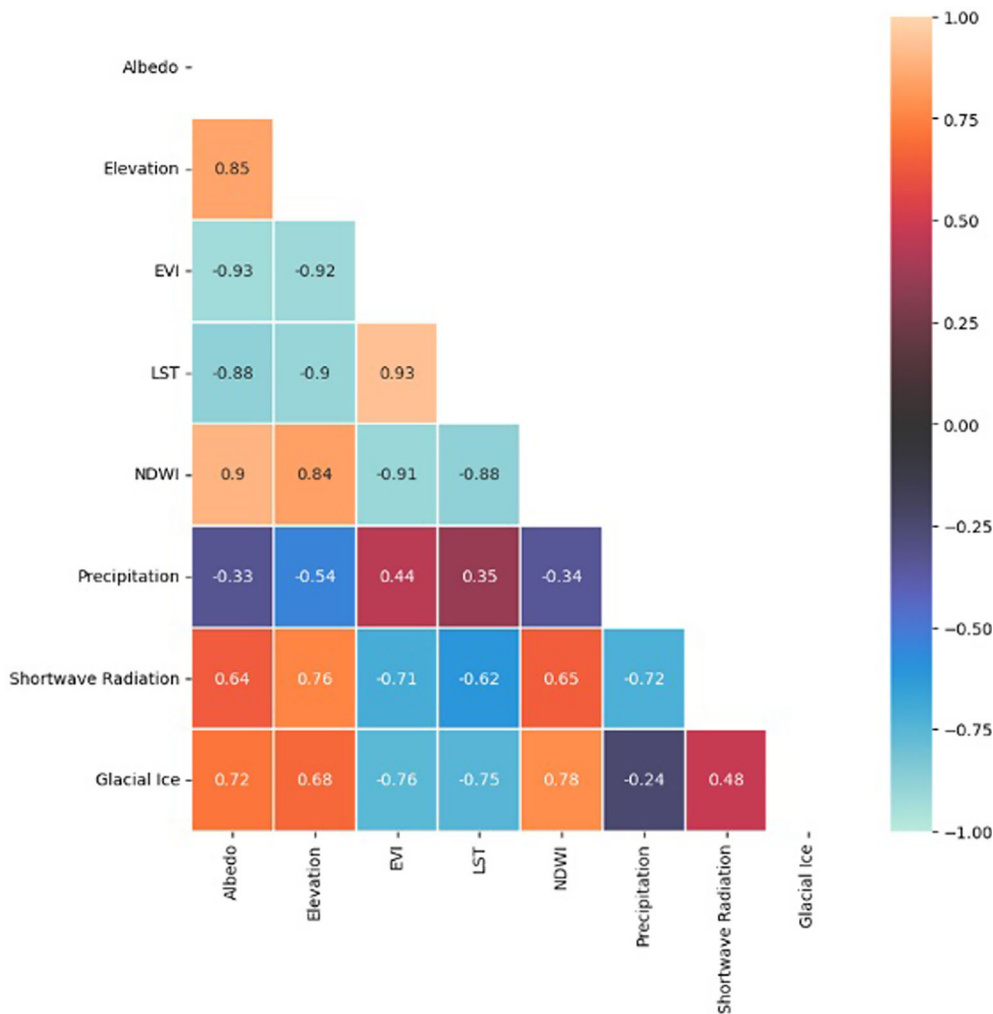


Figure 2. Influencing correlation between different parameters.

into glacial ice. Albedo, which may not deviate considering water surfaces to a significant extent, the angle of incidence of radiation has proven to be effective in giving higher deviation (Angstrom 1925), and given the waters in the surrounding area are at freezing temperatures, the wavelength of radiation emitted radiation from the water surface can be higher, as can be seen in the strong similarity in trend lines that albedo and NDSI share with NDWI. Considering vegetation, albedo varies w.r.t. type of vegetation, but on average returns lesser values to most vegetation types (Karthikeyan *et al.* 2019), thus the inverse trend lines that they share. There is a strong similarity in the trend lines of albedo in figure 4 and that of RSDN as previously established.

RSDN and LST share similarities in trend lines since the presence of radiation in the atmosphere increases the temperature in the surrounding area (Calleja *et al.* 2021).

4. Models and methodology

The study focuses on the identification of the best-fit model for modelling glacial retreat over the region. Three separate models, i.e., three of the most common models used within Machine Learning and Deep Learning studies – Feedforward Artificial Neural Networks (ANN), Recurrent Neural Networks (RNN) and Long-Short Term Memory (LSTM) are considered for the identification of the best-fit model for glacial delineation. Function optimization is a vital factor to consider, to minimize the overall network error. One such method is Levenberg Marquardt (LM), which has recently been adapted to a great degree by engineers, researchers and scientists as it provides an efficient method since it is a combination of the Gauss–Newton algorithm (speed) and the steepest gradient decent method (stability) (Sharifahmadian 2015). Due to its performance and handling

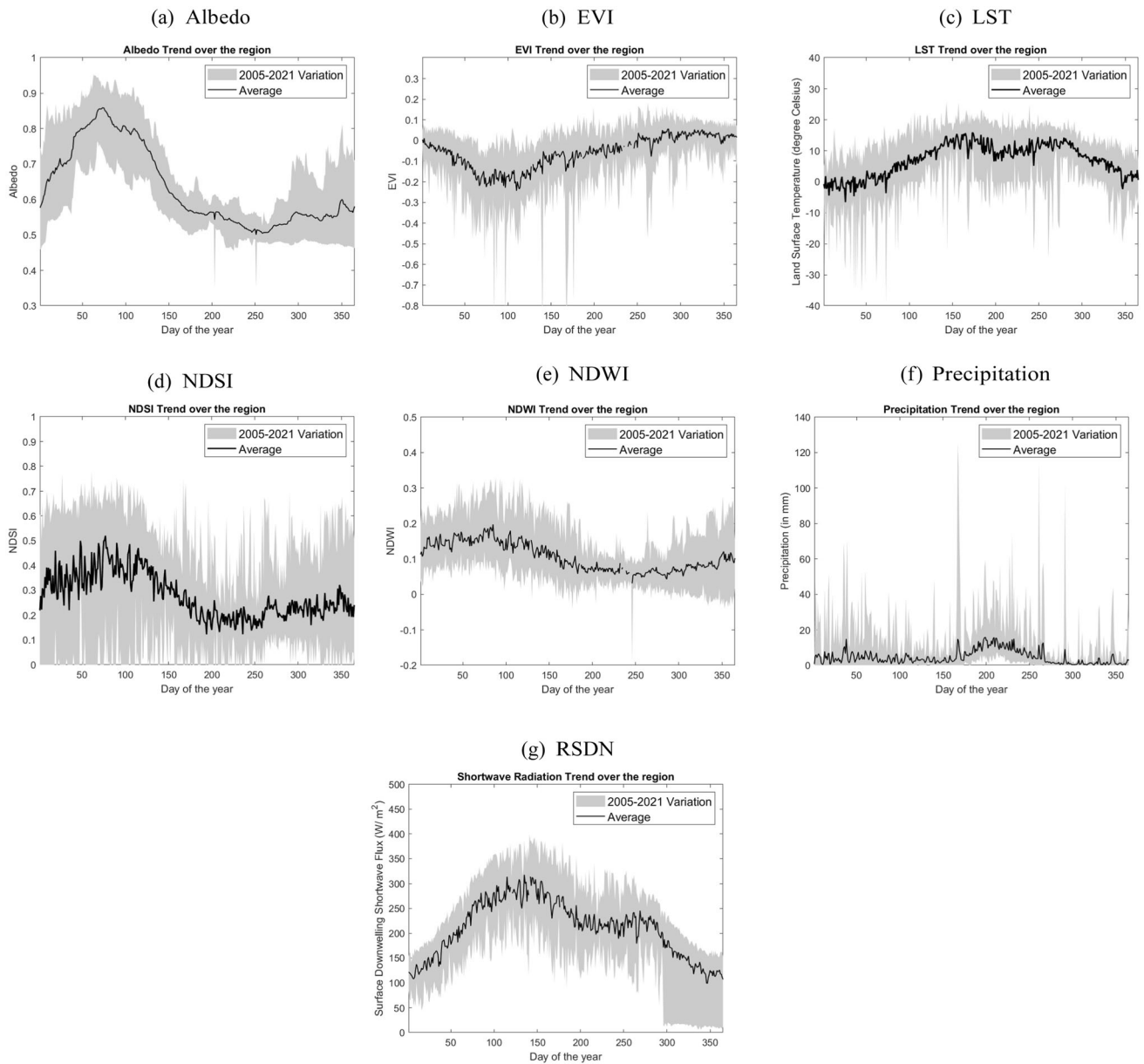


Figure 3. Trend variation of parameters: (a) Albedo, (b) enhanced vegetation index, (c) land surface temperature, (d) normalized difference snow index, (e) normalized difference water index, (f) precipitation, and (g) shortwave downwelling flux.

capabilities, LM is being used for meteorological applications, and ecological and biological assessments (Ferreira *et al.* 2011). The algorithm accurately estimates the desired outputs by generating the sum square error for evaluation. The LM-backpropogation (BP), on the other hand, compensates for the number of hidden layers based on the partial derivatives which are used to improve the performance of the gradient descent based on the Jacobian matrix. The LM derivates the nonlinear function between the input neuron and output based on the activation function (Janowski and Duch 2001). The net input (net_j)

projects the dataset based on the non-linearity necessary to estimate the desired measurements. Every activation function (or non-linearity) accepts a single number and performs a precise fixed mathematical operation on it (Ramachandran *et al.* 2017). The model was trained with 1000 iterations, while the condition was kept for the model to stop training provided it reached the global minimum of error prior to the completion of iterations. For proper comparative purposes, the number of hidden layers, nodes, activation and training-validation datasets have been kept the same. Each architecture has five hidden layers with

128, 246, 512, 256, and 128; the number of hidden nodes following the $2n - 1$ rule suggested by Heaton. Along with the same, the symmetry between each side of the middle-hidden layer has been kept the same for better approximation (Heaton 2008). The activation functions are a combination of tanh and ReLU as they provide a better approximation for regression-centric studies (Pomerat *et al.* 2019). The parameters for model evaluation include mean square error (MSE) and root mean square error (RMSE) along with the regression accuracy, after which the best model is tested with a dataset of a differing temporal range for its validation, using the same metrics of MSE, RMSE and accuracy over 1000 iterations. The temporal range of the dataset is between 2005 and 2021, of which the datasets have been divided into a 70:30 ratio randomly prior to model training.

4.1 Artificial Neural Network (ANN)

Feedforward ANN or Multilayer Perception (MLP) (depicted in figure 4) is the most common neural network whose structure resembles that of the human brain (Popescu *et al.* 2009; Ramchoun *et al.* 2016), wherein the transmission of signals occurs unidirectionally from Input (I/P) to Output (O/P). The neurons themselves remain unaffected by their O/P without the presence of any loop, which makes it a feedforward architecture (Popescu *et al.* 2009). A nonlinear function is generated via the architecture that allows for the prediction of O/P given the I/P data. Feedforward ANNs, however, are limited to classifications of the

static kind for mapping I/P to generate the O/P; time-series data necessitate more dynamicity than made available by ANN architectures (Staudemeyer and Morris 2019).

4.2 Recurrent Neural Network (RNN)

RNN, contrary to the feedforward architecture of the ANN, has closed-loop feedback connections that are designed for sequential data through processing real sequences step by step for the prediction of the next in the sequence (Fausett 1994; Medsker and Jain 2001; Graves 2013) as depicted in figure 5.

Similar to ANN, RNNs have distinct I/P, O/P and hidden layers that are interconnected with their respective weights, biases and activations, but ones that are interconnected partially or fully depending on the intended architecture of the RNN model (Medsker and Jain 2001). The predictions from an RNN, however, are generated not from the input training data itself but the multi-dimensional interpolation made from the model's own 'understanding' of the data, the predictions themselves being derived from matches between the training data and the input dataset for prediction (Graves 2013). RNNs are able to 'memorize' earlier events as they process current data due to the presence of their internal state at each iteration and the circular or recurrent connections to the lower and higher layers of neurons. RNNs are, however, limited to looking back nearly 10 timesteps due to the vanishing fed-back signal (Staudemeyer and Morris 2019).

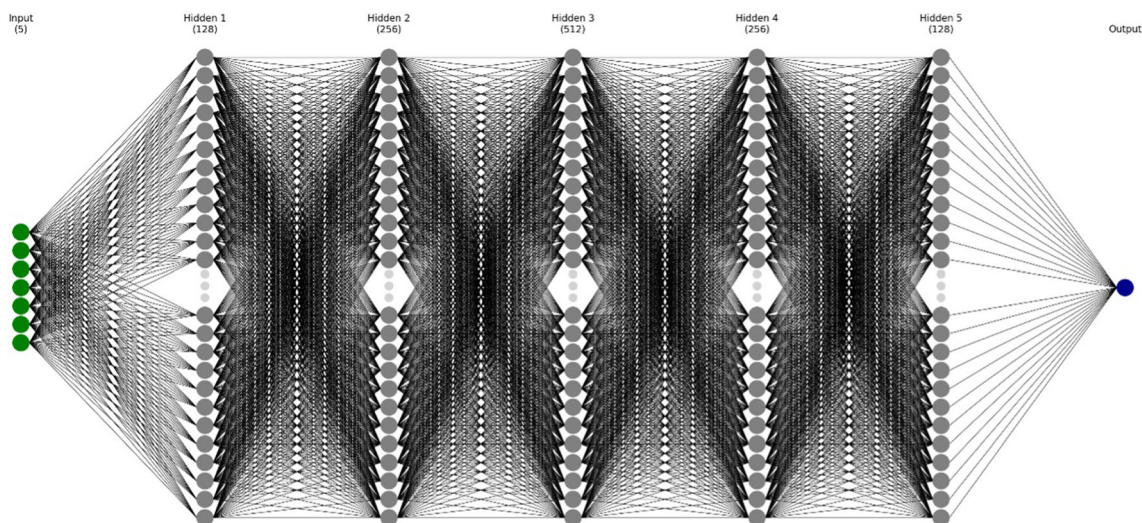


Figure 4. ANN architecture used in the study.

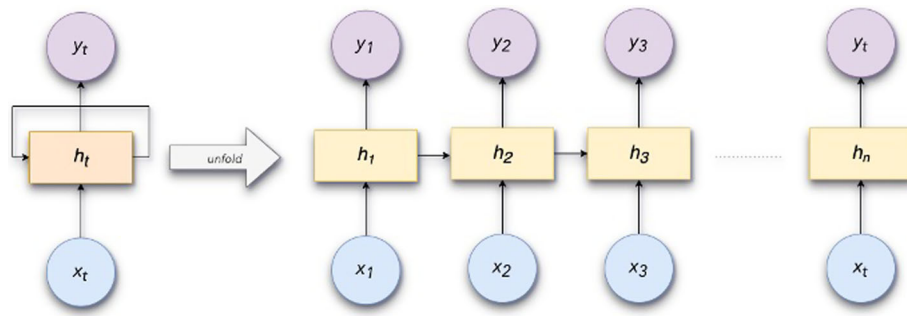


Figure 5. Typical architecture of a RNN (Son and Kim 2020).

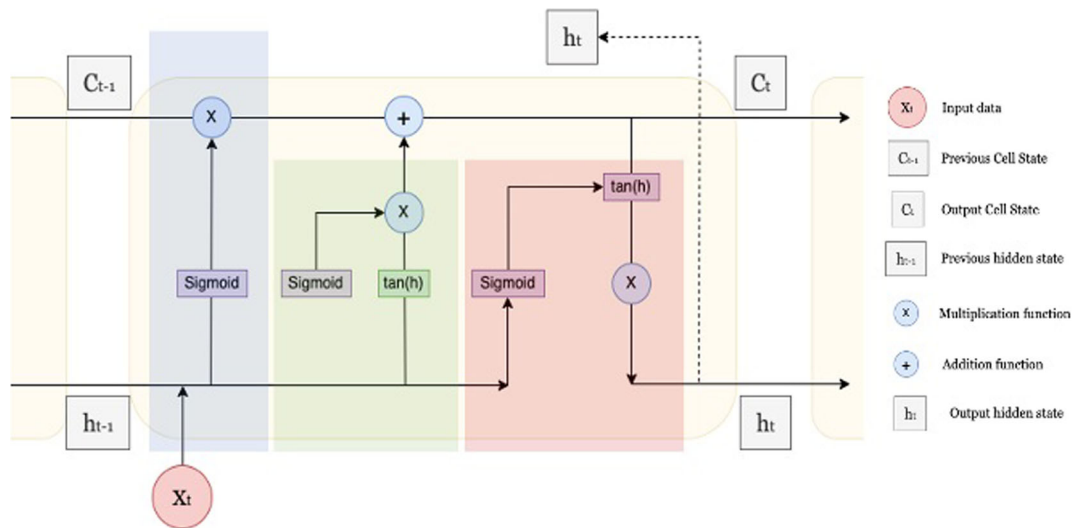


Figure 6. Typical architecture of an LSTM cell (Lazaris and Prasanna 2020).

4.3 Long-Short Term Memory (LSTM)

LSTM or an LSTM-RNN is a variant of RNN architecture that addresses the long-term dependency problem and the lack of ANN’s ability to deal with sequential data adequately via memory cells that filter data out, cell-by-cell, as depicted in figure 6.

It allows for bridging of time gaps of over a thousand by allowing for a consistent error flow within the specialized versions of the RNN cells, the access to and exit from which being handled by gates that regularize the cell-to-cell data access (Staudemeyer and Morris 2019). Each LSTM cell has three cells: the forget gate, the I/P gate and the O/P gate. The forget gate allows for the filtering of information as to which information enters the cell through the sigmoid function; tanh adds weights to the information, which then passes through the I/P gate that decides which information is stored in the cell, and the O/P gate deciding which information

leaves the cell, in both instances, through sigmoid that filters out the values and tanh that adds weights, similar to the forget gate. It is through this mechanism that LSTM can retain the necessary information while ‘forgetting’ the irrelevant past information. An additional layer that LSTM adds to RNN is the states; the hidden state is the information that is passed to the cell from the immediately preceding cell that also backpropagates for prediction purposes, while the cell state is all the previously remembered information (Staudemeyer and Morris 2019).

5. Model performance and results

The models were trained on a 70–30 split of data division, with a 1000-epoch limit, to consider a standard for comparison and the results are shown in figure 7. It was observed that the accuracy of ANN has saturated at 62.35% while the RMSE

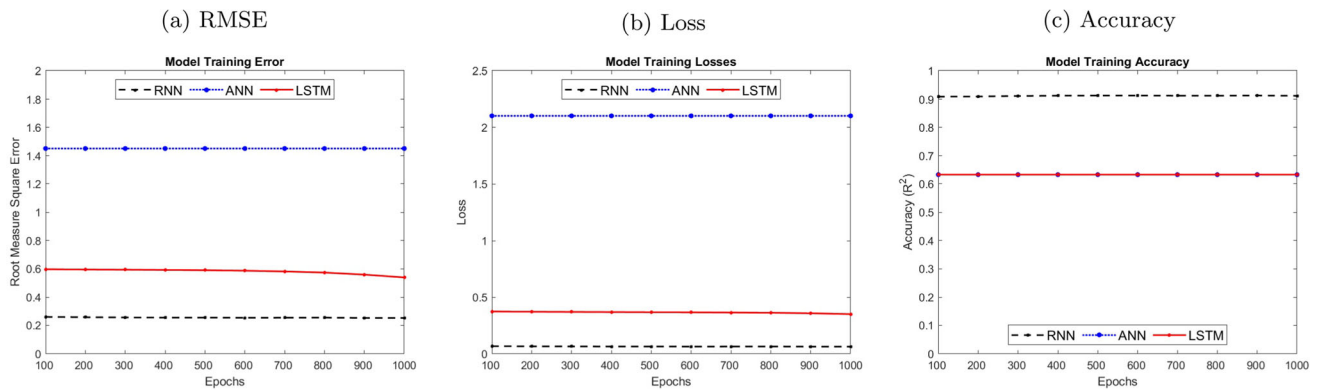


Figure 7. Model performance matrix evaluation for (a) RMSE, (b) loss and (c) accuracy.

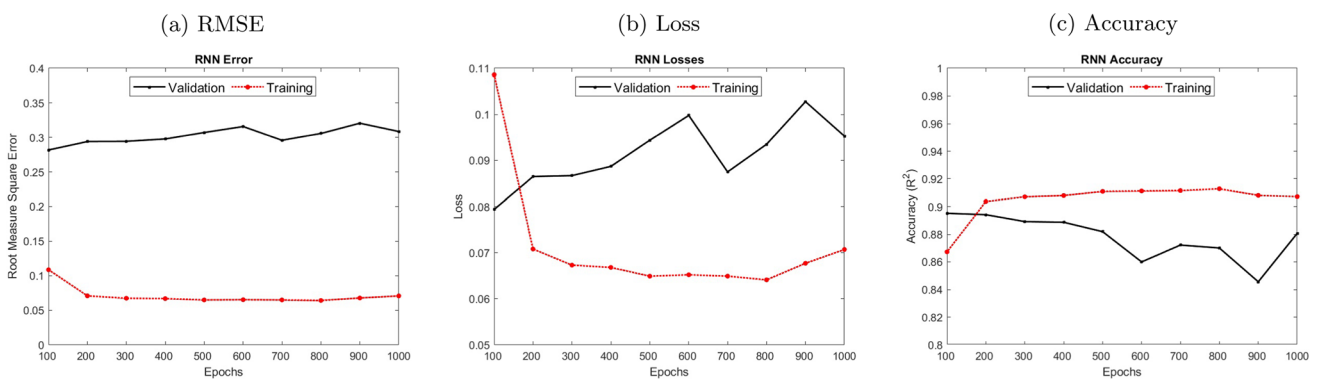


Figure 8. RNN model performance during training and validation for (a) RMSE, (b) loss and (c) accuracy.

remains unchanged at the high value of 1.45 and MSE at 2.1. On the other hand, LSTM provided a similar accuracy performance; however, the error continues to reduce. RNN provided the best performance across the three with an accuracy score of 0.9, RMSE of 0.27 and MAE of 0.07, the performances are shown in figure 7. The RNN trends are depicted in figure 8.

From the temporal graphs depicted above, the shortcoming within the ANN point made in Staudemeyer and Morris (2019) regarding the need for a dynamicity for time series data that ANN does not exhibit has been proven in the instance. RNN performed well given its feedback mechanism properties and can reliably assist in the processing of long-term sequential data (Mou *et al.* 2017), unlike the ANN, which is unable to realize the inherent dependencies between sequential inputs (Sharma *et al.* 2018). For multi-temporal and spectral data that has been used in the study, RNN's structure allows for connections between hidden layers without any time delay, enables better dealing with the inherent dependencies,

counter to the multilayer dense structure of an ANN that cannot deal with the same (Lakhal *et al.* 2018). It is necessary to note here that despite LSTM being cited to be better suited to temporal and multi-spectral data in comparison to a standard RNN (Ienco *et al.* 2017; Lakhal *et al.* 2018; Sharma *et al.* 2018) given that LSTM provides a solution to the vanishing or exploding gradient that standard RNNs have an issue with Mou *et al.* (2017) and Ndikumana *et al.* (2018). However, in the case of this study, standard RNN has given better results than the oversaturated LSTM. Moreover, LSTM saturates to the same performance level as the ANN. This can be attributed to the target of binary classification during the training phase. While LSTM is better as a model, the binary classifier problem cannot be directly quantified for both feedforward and LSTM models (Li *et al.* 2017). RNN model, however, due to its lacking dependencies within the structure as well as the gradient approach included, can be the reason why it performed, nonetheless. The RNN architecture is such that while being simpler in

reference when compared to the LSTM design, it can perform better under specific conditions. One of the key aspects is the data characteristics; this is a major shortcoming of LSTM (Sherstinsky 2020) as the variations are significantly influenced by the short-term period over the land term due to the timescale considered. The very advantage of LSTM is leading to its shortcoming in the performance. Secondly, the feature representation, the features extracted from the glacial data, might not require the sophisticated memory mechanism of the LSTMs (Rahmani *et al.* 2021). Since the information needed for accurate delineation can be effectively captured by a model with simpler temporal dependencies, RNN is sufficient. Lastly, the training data size, while the LM-BP was deployed, presents a possibility of generalization within the model. The increased number of parameters may not necessarily be needed when it comes to the amount of and scale of datasets being used over the region (Bhatia 2022).

6. Glacial boundary delineation

The glacial extent for each year within the temporal range of observation was derived from the best-fit model (which includes the training and validation periods). The figures that follow are the maps for the aforementioned glacial extents. The predictions from each year have been used for the glacial change detection and a boundary delineation was derived and depicted in figure 9.

Furthermore, the temporal area derivations from the same, plotted in figure 9, show a breathing pattern observation due to the shift in atmospheric rivers. Whilst the overall trend is decreasing, the extent of glaciers is still varying by a significant extent year by year, which is not in a solely decreasing fashion. This is the breathing effect of the glaciers; the glacial–interglacial cycles are influenced to a significant extent by the ENSO oscillations (Tudhope *et al.* 2001). El Niño implies warmer water spreads further, thus releasing more heat into the atmosphere, while La Niña wind and precipitation are influenced heavily despite the average temperatures in a region (Trenberth 1997). Precipitation, water extent, surface temperature, wind direction and wind speed are heavily influenced by the ENSO cycles (McCreary 1976; Tudhope *et al.* 2001). As in figure 10, the breathing pattern of the ROI glacial extent observes an increase every three years, then observes a decline

in the extent for three years. A glacial maximum is observed in 3-year intervals, and thus in 2022, the glacial extent is expected to decrease given the trend line. The model, thus developed, can be used to identify such conditions within the boundaries of different glaciers.

Within the validation dataset, five-time periods were extracted, and a change within the boundaries of the potential glacier can be observed in figure 10. A direct reduction in the overall snow cover within the span of 15 years can be observed. Trend lines have been identified for the observation of the breathing pattern of the glacier. Albeit the large fluctuations, the trend line suggests a gradual retreat in the glacier, as in figure 9. It can be observed that in each instance of the glacial ice reduction from year to year, the decrease is parallel to the trend line. The study can be further scaled to the prediction of the glacial extent of various glaciers and temporal ranges for the glacial delineation studies. This can help with the decision-making for local bodies in dealing with the *in-situ* situations and respond accordingly to extreme situations, such as the Chorabari GLOF in 2013 (Rafiq *et al.* 2019), landslides due to the glaciers and rested pond on-site or a policy level; reducing ice sheet levels, the decrease in freshwater on land due to melting ice sheets pouring the glacial freshwater into the ocean, shifting oceanic currents in the process and so forth – various glacial climate phenomena may be modelled and identified through the approach undertaken in the study.

7. Discussion and way forward

The study highlights the breathing and variations within the region. Some aspects need to be accounted for, when considering the underlying influences to mitigate the future. The region is strongly influenced by climate change by a combination of natural and human-induced factors. One of the key drivers is the overall rise in global temperatures. Warmer temperatures contribute to increased melting of glaciers, leading to a reduction in glacial mass and size over time (Kraaijenbrink *et al.* 2017). Secondly, the emission of greenhouse gases, such as carbon dioxide and methane, contributes to the enhanced greenhouse effect, trapping heat in the Earth's atmosphere. This warming effect accelerates glacial melting in the Himalayan region. Along with the same, particles like black carbon (soot) deposited on the glacier surface

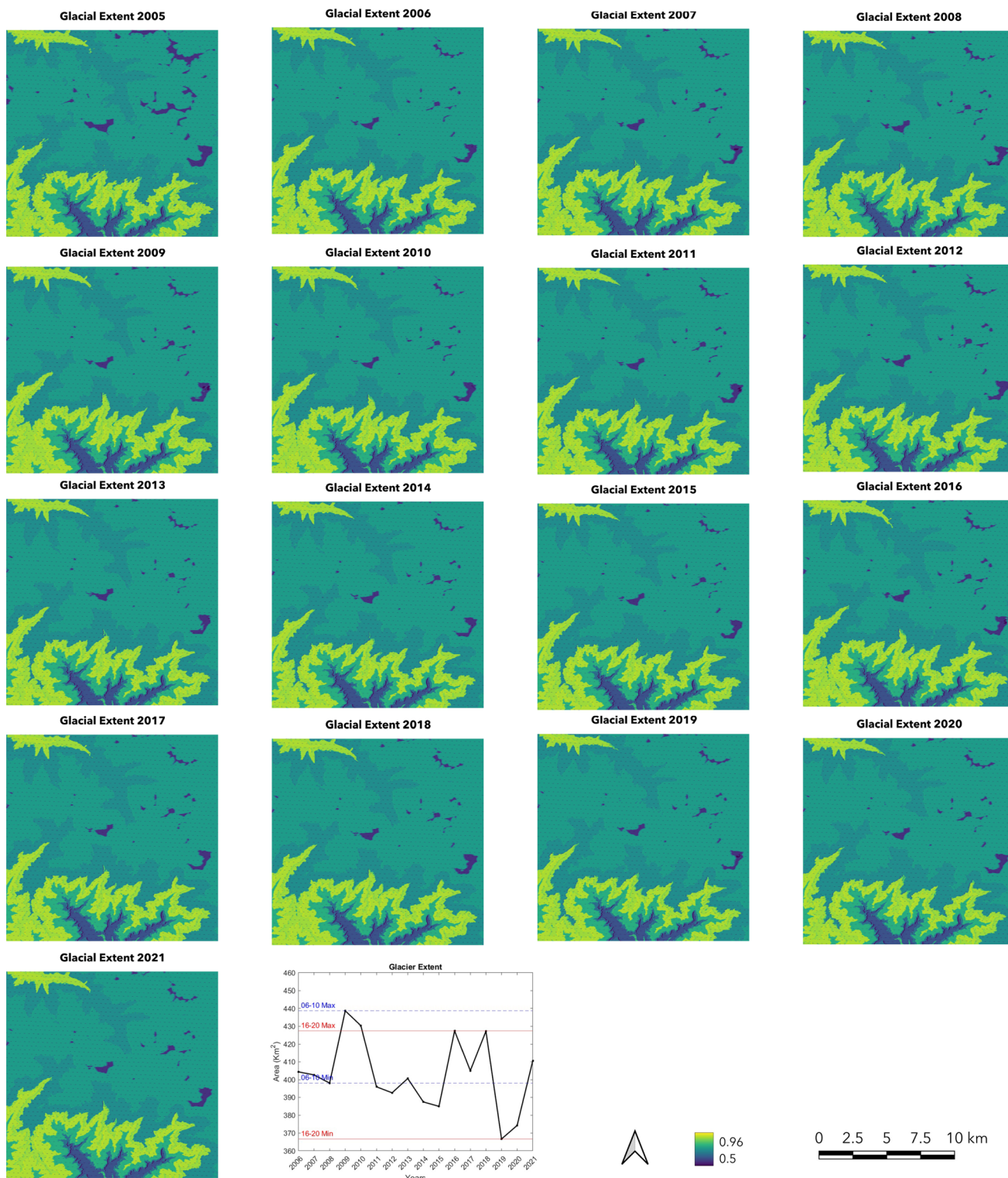


Figure 9. Model derived annual glacier boundary extent over the span of 2005–2021 and the variations in the overall area (bottom right).

absorb sunlight, reducing the glacier’s albedo (reflectivity) and accelerating the melting process. This is often linked to industrial and biomass-burning activities (Kumar *et al.* 2021a, b). This may also lead to alterations in precipitation

patterns, such as changes in the form (rain *vs.* snow) and timing of precipitation, which can impact glacier mass balance. If more precipitation falls as rain rather than snow, it can lead to faster melting. The Himalayan region is influenced by

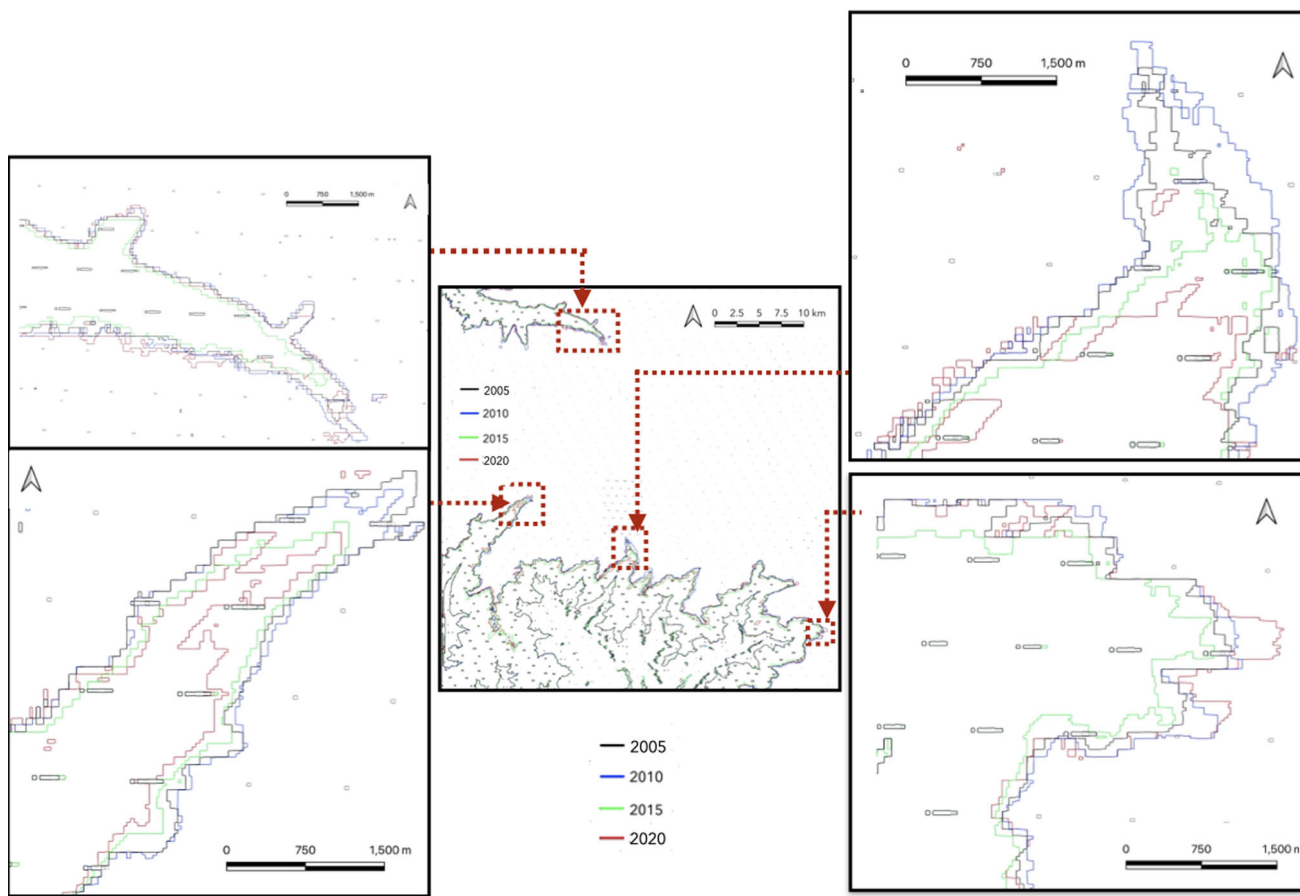


Figure 10. 5-year temporal interval variations in glacier extent over the region.

complex climatic systems. Changes in atmospheric circulation patterns and regional climate variability can affect the temperature and precipitation regimes, influencing glacial dynamics (Singh and Bengtsson 2004). Lastly, human activities, such as deforestation and urbanization, can influence local climate conditions and indirectly impact glaciers. Changes in land use can alter the albedo and heat absorption properties of the landscape (Massad *et al.* 2019). Understanding these drivers is crucial for developing effective strategies to mitigate the impacts of glacial retreat and address the broader issue of climate change. It requires both global efforts to reduce greenhouse gas emissions and regional initiatives to adapt to the changing environment.

The current study does not directly account for the underlying drivers for the region. The future aspect of the same can consider these influences directly, while suggesting possible mitigation, adaptive and transformative strategies like higher reliance on solar potential to reduce hydroelectric dependencies. Better tourism policies to reduce the amount of human influence over the region and considering integrating reinforced nature-based

land use within the built forms to counterbalance the loss of ecosystem serve as a barrier for landslide and GLOF-infused calamities.

8. Conclusion

A study focused on observing the spatio-temporal variations in glacial land use, through which a machine learning model was developed to observe the patterns of retreat in the glacier. Three commonly used machine learning models were compared – ANN, RNN and LSTM and through the results, it was concluded that RNN is the best-fit for the current study as it outperformed the other two models by an R^2 of roughly 0.3. Furthermore, RNN was used for glacial boundary delineation to observe the pattern of change in the glacier. The ROI, which encompasses various glaciers, including Chorabari and Gangotri glaciers, has been observed to have an average extent of 403 km², over a span of 2342 km². The model can be further scaled for the prediction of the glacial extent of different glaciers over various temporal ranges for

the glacial delineation studies. This can help with the decision-making of local bodies in dealing with *in-situ* situations and responding accordingly to extreme situations.

Acknowledgements

The authors would like to thank the Faculty of Technology, CEPT University and CEPT University management for providing the infrastructure and support to carry out this study.

Author statement

Sriram focused on data collection, data processing, development, validation of the models and drafted the manuscript. Dhwanilnath guided, supervised the analysis, model development as well as drafted and edited the manuscript. Shaily guided and supervised the analysis.

References

- Angstrom A 1925 The albedo of various surfaces of ground; *Geografiska Annaler* **7(4)** 323–342, <https://doi.org/10.1080/20014422.1925.11881121>.
- Baraka S, Akeru B, Aryal B, Sherpa T, Shrestha F, Ortiz A and Bengio Y 2020 Machine learning for glacier monitoring in the Hindu Kush Himalaya; <https://doi.org/10.48550/arXiv.2012.05013>.
- Bhambri R, Bolch T and Chaujar R K 2012 Frontal recession of Gangotri Glacier, Garhwal Himalayas, from 1965 to 2006, measured through high-resolution remote sensing data; *Curr. Sci.* **102(3)** 489–494.
- Bhatia Y 2022 Bi-modal deep neural network for gait emotion recognition; Master's thesis, University of Calgary, Calgary, Canada.
- Bolibar J, Rabatel A, Gouttevin I, Galiez C, Condom T and Sauquet E 2020 Deep learning applied to glacier evolution modelling; *Cryosphere* **14(2)** 565–584, <https://doi.org/10.5194/tc-14-565-2020>.
- Calleja J F, Muñiz R, Fernandez S, Corbea-Pérez A, Peón J, Otero J and Navarro F 2021 Snow albedo seasonal decay and its relation with shortwave radiation, surface temperature and topography over an Antarctic ice cap; *IEEE J. Sel. Top. Appl. Earth Observ. Remote Sens.* **14** 2162–2172, <https://doi.org/10.1109/JSTARS.2021.3051731>.
- Carey M, Molden O C, Rasmussen M B, Jackson M, Nolin A W and Mark B G 2017 Impacts of glacier recession and declining meltwater on mountain societies; *Ann. Am. Assoc. Geogr.* **107(2)** 350–359.
- Church J A, Clark P U, Cazenave A, Gregory J M, Jevrejeva S and Levermann A *et al.* 2013 Sea-level rise by 2100; *Science* **342(6165)** 1445, <https://doi.org/10.1126/science.342.6165.1445-a>.
- Das P K 2013 The Himalayan tsunami-cloudburst, flash flood and death toll: A geographical postmortem; *IOSR-JESTFT* **7(2)** 33–45.
- Dubey S and Goyal M K 2020 Glacial lake outburst flood hazard, downstream impact, and risk over the Indian Himalayas; *Water Resour. Res.* **56(4)** e2019WR026533, <https://doi.org/10.1029/2019WR026533>.
- Fausett L 1994 *Fundamentals of neural networks*; Prentice Hall, Englewood Cliffs, NJ.
- Ferreira A G, Soria-Olivas E, Lopez A J S and Lopez-Baeza E 2011 Estimating net radiation at surface using artificial neural networks: A new approach; *Theor. Appl. Climatol.* **106** 263–279, <https://doi.org/10.1007/s00704-011-0488-7>.
- Gao S 2020 A review of recent researches and reflections on geospatial artificial intelligence; *Geomat. Inf. Sci. Wuhan Univ.* **45(12)** 1865–1874, <https://doi.org/10.13203/j.whugis20200597>.
- Garrard R, Kohler T, Price M F, Byers A C, Sherpa A R and Maharjan G R 2016 Land use and land cover change in Sagarmatha National Park, a world heritage site in the Himalayas of eastern Nepal; *MT. Res. Dev.* **36(3)** 299–310, <https://doi.org/10.1659/MRD-JOURNAL-D-15-00005.1>.
- Ghatak D, Sinsky E and Miller J 2014 Role of snow-albedo feedback in higher elevation warming over the Himalayas, Tibetan Plateau and Central Asia; *Environ. Res. Lett.* **9(11)** 114008, <https://doi.org/10.1088/1748-9326/9/11/114008>.
- Graves A 2013 Generating sequences with recurrent neural networks; <https://doi.org/10.48550/arXiv.1308.0850>.
- Guidicelli M, Huss M, Gabella M and Salzmann N 2023 Spatio-temporal reconstruction of winter glacier mass balance in the Alps, Scandinavia, central Asia and western Canada (1981–2019) using climate reanalyses and machine learning; *Cryosphere* **17(2)** 977–1002, <https://doi.org/10.5194/tc-17-977-2023>.
- Heaton J 2008 *Introduction to neural networks with Java*; Heaton Research, Inc.
- Hock R 2005 Glacier melt: A review of processes and their modelling; *Progr. Phys. Geogr.* **29(3)** 362–391, <https://doi.org/10.1191/0309133305pp453ra>.
- Ienco D, Gaetano R, Dupaquier C and Maurel P 2017 Land cover classification via multitemporal spatial data by deep recurrent neural networks; *IEEE Geosci. Remote Sens. Lett.* **14(10)** 1685–1689, <https://doi.org/10.1109/LGRS.2017.2728698>.
- Jain S K, Lohani A K, Singh R, Chaudhary A and Thakural L 2012 Glacial lakes and glacial lake outburst flood in a Himalayan basin using remote sensing and GIS; *Nat. Hazards* **62** 887–899, <https://doi.org/10.1007/s11069-012-0120-x>.
- Jankowski N and Duch W 2001 Optimal transfer function neural networks; ESANN 2001, 9th European Symposium on Artificial Neural Networks, Bruges, Belgium, April 25–27, 2001, pp. 101–106.
- Jury M W, Mendlik T, Tani S, Truhetz H, Maraun D, Immerzeel W W and Lutz A F 2020 Climate projections for glacier change modelling over the Himalayas; *Int. J. Climatol.* **40(3)** 1738–1754, <https://doi.org/10.1002/joc.6298>.
- Kadota T, Fujita K, Seko K, Kayastha R B and Ageta Y 1997 Monitoring and prediction of shrinkage of a small glacier in the Nepal Himalaya; *Ann. Glaciol.* **24** 90–94, <https://doi.org/10.3189/S0260305500011988>.

- Kamel Boulos M N, Peng G and VoPham T 2019 An overview of geoi applications in health and healthcare; *Int. J. Health Geogr.* **18** 1–9, <https://doi.org/10.1186/s12942-019-0171-2>.
- Karthikeyan L, Pan M, Konings A G, Piles M, Fernandez-Moran R, Kumar D N and Wood E F 2019 Simultaneous retrieval of global scale vegetation optical depth, surface roughness, and soil moisture using x-band AMSR-E observations; *Rem. Sens. Environ.* **234** 111473, <https://doi.org/10.1016/j.rse.2019.111473>.
- Kaushik S, Dharpure J K, Joshi P, Ramanathan A and Singh T 2020 Climate change drives glacier retreat in Bhaga Basin located in Himachal Pradesh, India; *Geocarto Int.* **35**(11) 1179–1198, <https://doi.org/10.1080/10106049.2018.1557260>.
- Khanal N R, Mool P K, Shrestha A B, Rasul G, Ghimire P K, Shrestha R B and Joshi S P 2015 A comprehensive approach and methods for glacial lake outburst flood risk assessment, with examples from Nepal and the transboundary area; *Int. J. Water Res. Dev.* **31**(2) 219–237, <https://doi.org/10.1080/07900627.2014.994116>.
- Kraaijenbrink P D, Bierkens M F, Lutz A F and Immerzeel W 2017 Impact of a global temperature rise of 1.5 degrees celsius on Asia's glaciers; *Nature* **549**(7671) 257–260, <https://doi.org/10.1038/nature23878>.
- Kulkarni A V, Bahuguna I, Rathore B, Singh S, Randhawa S, Sood R and Dhar S 2007 Glacial retreat in Himalaya using Indian remote sensing satellite data; *Curr. Sci.* **92**(1) 69–74.
- Kumar V, Ranjan D and Verma K 2021a Global climate change: The loop between cause and impact; In: *Global climate change*, Elsevier, pp. 187–211.
- Kumar V, Shukla T, Mehta M, Dobhal D, Bisht M P S and Nautiyal S 2021b Glacier changes and associated climate drivers for the last three decades, Nanda Devi region, central Himalaya, India; *Quat. Int.* **575** 213–226, <https://doi.org/10.1016/j.quaint.2020.06.017>.
- Kusky T M 2010 *Climate change: Shifting glaciers, deserts, and climate belts*; Infobase Publishing.
- Lakhal M I, Çevikalp H, Escalera S and Offi F 2018 Recurrent neural networks for remote sensing image classification; *IET Comput. Vis.* **12**(7) 1040–1045, <https://doi.org/10.1049/iet-cvi.2017.0420>.
- Lazaris A and Prasanna V K 2020 An LSTM framework for software-defined measurement; *IEEE Trans. Netw. Serv. Manag.* **18**(1) 855–869, <https://doi.org/10.1109/TNSM.2020.3040157>.
- Li X, Zhang Y, Zhang J, Chen S, Marsic I, Farneth R A and Burd R S 2017 Concurrent activity recognition with multimodal CNN-LSTM structure; <https://doi.org/10.48550/arXiv.1702.01638>.
- Massad R S, Lathière J, Strada S, Perrin M, Personne E, Stéfano M and de Noblet-Ducoudré N 2019 Reviews and syntheses: Influences of landscape structure and land uses on local to regional climate and air quality; *Biogeosciences* **16**(11) 2369–2408, <https://doi.org/10.5194/bg-16-2369-2019>.
- McCarthy J 2007 *What is artificial intelligence*; <http://www-formal.stanford.edu/jmc/>.
- McCreary J 1976 Eastern tropical ocean response to changing wind systems: With application to El Niño; *J. Phys. Oceanogr.* **6**(5) 632–645, [https://doi.org/10.1175/1520-0485\(1976\)006<0632:ETORTC>2.0.CO;2](https://doi.org/10.1175/1520-0485(1976)006<0632:ETORTC>2.0.CO;2).
- Medsker L R and Jain L 2001 Recurrent neural networks; *Design Appl.* **5** 64–67.
- Mehta M, Majeed Z, Dobhal D and Srivastava P 2012 Geomorphological evidences of post-LGM glacial advancements in the Himalaya: A study from Chorabari Glacier, Garhwal Himalaya, India; *J. Earth Syst. Sci.* **121** 149–163, <https://doi.org/10.1007/s12040-012-0155-0>.
- Mehta M, Dobhal D, Kesarwani K, Pratap B, Kumar A and Verma A 2014 Monitoring of glacier changes and response time in Chorabari glacier, central Himalaya, Garhwal, India; *Curr. Sci.* **107**(2) 281–289.
- Mou L, Ghamisi P and Zhu X X 2017 Deep recurrent neural networks for hyperspectral image classification; *IEEE Trans. Geosci. Remote Sens.* **55**(7) 3639–3655, <https://doi.org/10.1109/TGRS.2016.2636241>.
- Ndikumana E, Ho Tong Minh D, Baghdadi N, Courault D and Hossard L 2018 Deep recurrent neural network for agricultural classification using multitemporal Sar Sentinel-1 for Camargue, France; *Remote Sens.* **10**(8) 1217, <https://doi.org/10.3390/rs10081217>.
- Patel L K, Sharma P, Fathima T and Thamban M 2018 Geospatial observations of topographical control over the glacier retreat, Miya Basin, Western Himalaya, India; *Environ. Earth Sci.* **77** 1–12, <https://doi.org/10.1007/s12665-018-7379-5>.
- Pellicciotti F, Brock B, Strasser U, Burlando P, Funk M and Corripio J 2005 An enhanced temperature-index glacier melt model including the shortwave radiation balance: Development and testing for Haut Glacier D'arolla, Switzerland; *J. Glaciol.* **51**(175) 573–587, <https://doi.org/10.3189/172756505781829124>.
- Pellikka P and Rees W G 2009 *Remote sensing of glaciers: Techniques for topographic, spatial and thematic mapping of glaciers*; CRC Press.
- Pomerat J, Segev A and Datta R 2019 On neural network activation functions and optimizers in relation to polynomial regression; *2019 IEEE International Conference on Big Data (big data)*, pp. 6183–6185.
- Popescu M-C, Balas V E, Perescu-Popescu L and Mastorakis N 2009 Multilayer perceptron and neural networks; *WSEAS Trans. Circuits Syst.* **8**(7) 579–588.
- Rafiq M, Romshoo S A, Mishra A K and Jalal F 2019 Modelling Chorabari lake outburst flood, Kedarnath, India; *J. Mt. Sci.* **16**(1) 64–76, <https://doi.org/10.1007/s11629-018-4972-8>.
- Rahmani F, Lawson K, Ouyang W, Appling A, Oliver S and Shen C 2021 Exploring the exceptional performance of a deep learning stream temperature model and the value of streamflow data; *Environ. Res. Lett.* **16**(2) 024025, <https://doi.org/10.1088/1748-9326/abd501>.
- Rajagopalan G 2021 Data visualization with Python libraries. A Python Data Analyst's Toolkit: Learn Python and Python-based Libraries with applications in data analysis and statistics, pp. 243–278, https://doi.org/10.1007/978-1-4842-6399-0_7.
- Ramachandran P, Zoph B and Le Q V 2017 Searching for activation functions; <https://doi.org/10.48550/arXiv.1710.05941>.
- Ramchoun H, Ghanou Y, Eттаouil M and Janati Idrissi M A 2016 Multilayer perceptron: Architecture optimization and training; <https://doi.org/10.9781/ijimai.2016.415>.
- Rees W G 2005 *Remote sensing of snow and ice*; CRC Press.

- Romshoo S A and Rashid I 2010 Potential and constraints of geospatial data for precise assessment of the impacts of climate change at landscape level; *Int. J. Geomat. Geosci.* **1(3)** 386–405.
- Romshoo S A, Murtaza K O, Shah W, Ramzan T, Ameen U and Bhat M H 2022 Anthropogenic climate change drives melting of glaciers in the Himalaya; *Environ. Sci. Pollut. Res.* **29(35)** 52,732–52,751, <https://doi.org/10.1007/s11356-022-19524-0>.
- Saikawa E, Panday A, Kang S, Gautam R, Zusman E, Cong Z and Adhikary B 2019 Air pollution in the Hindu Kush Himalaya; In: *The Hindu Kush Himalaya assessment: Mountains, climate change, sustainability and people*, pp. 339–387, https://doi.org/10.1007/978-3-319-92288-1_10.
- Sharifahmadian A 2015 *Numerical models for submerged breakwaters: Coastal hydrodynamics and morphodynamics*; Butterworth-Heinemann.
- Sharma A, Liu X and Yang X 2018 Land cover classification from multi-temporal, multi-spectral remotely sensed imagery using patch-based recurrent neural networks; *Neural Netw.* **105** 346–355, <https://doi.org/10.1016/j.neunet.2018.05.019>.
- Shea J, Immerzeel W, Wagnon P, Vincent C and Bajracharya S 2015 Modelling glacier change in the Everest region, Nepal Himalaya; *Cryosphere* **9(3)** 1105–1128, <https://doi.org/10.5194/tc-9-1105-2015>.
- Sherstinsky A 2020 Fundamentals of recurrent neural network (RNN) and long short-term memory (LSTM) network; *Phys. D: Nonlinear Phenomena* **404** 132306, <https://doi.org/10.1016/j.physd.2019.132306>.
- Singh P and Bengtsson L 2004 Hydrological sensitivity of a large Himalayan basin to climate change; *Hydrol. Process.* **18(13)** 2363–2385, <https://doi.org/10.1002/hyp.1468>.
- Singh R, Schickhoff U and Mal S 2016 *Climate change, glacier response, and vegetation dynamics in the Himalaya*; Springer International Publishing, Cham, Switzerland, <https://doi.org/10.1007/978-3-319-28977-9>.
- Son H and Kim C 2020 A deep learning approach to forecasting monthly demand for residential-sector electricity; *Sustainability* **12(8)** 3103, <https://doi.org/10.3390/su12083103>.
- Sood V, Tiwari R K, Singh S, Kaur R and Parida B R 2022 Glacier boundary mapping using deep learning classification over Bara Shigri Glacier in western Himalayas; *Sustainability* **14(20)** 13485, <https://doi.org/10.3390/su142013485>.
- Staudemeyer R C and Morris E R 2019 Understanding LSTM – a tutorial into long short-term memory recurrent neural networks; <https://doi.org/10.48550/arXiv.1909.09586>.
- Stephens G L, O'Brien D, Webster P J, Pilewski P, Kato S and Li J-L 2015 The albedo of Earth; *Rev. Geophys.* **53(1)** 141–163, <https://doi.org/10.1002/2014RG000449>.
- Stokes C R, Abram N J, Bentley M J, Edwards T L, England M H and Foppert A *et al.* 2022 Response of the East Antarctic ice sheet to past and future climate change; *Nature* **608(7922)** 275–286, <https://doi.org/10.1038/s41586-022-04946-0>.
- Taloor A J, Kothiyari G C, Manhas D R, Bisht H, Mehta P, Sharma M, Mahajan S, Roy S, Singh A K and Ali S 2021 Spatio-temporal changes in the Machoi glacier Zaskar Himalaya India using geospatial technology; *Quat. Sci. Adv.* **4** 100031, <https://doi.org/10.1016/j.qsa.2021.100031>.
- Trenberth K E 1997 The definition of El Niño; *Bull. Am. Meteorol. Soc.* **78(12)** 2771–2778, [https://doi.org/10.1175/1520-0477\(1997\)078<2771:TDOENO>2.0.CO;2](https://doi.org/10.1175/1520-0477(1997)078<2771:TDOENO>2.0.CO;2).
- Tripathi J N, Sonker I, Tripathi S and Singh A K 2022 Climate change traces on Lhonak Glacier using geospatial tools; *Quat. Sci. Adv.* **8** 100065, <https://doi.org/10.1016/j.qsa.2022.100065>.
- Tudhope A W, Chilcott C P, McCulloch M T, Cook E R, Chappell J, Ellam R M and Shimmield G B 2001 Variability in the El Niño-southern oscillation through a glacial-interglacial cycle; *Science* **291(5508)** 1511–1517, <https://doi.org/10.1126/science.1057969>.
- Yue X, Li Z, Zhao J, Fan J, Takeuchi N and Wang L 2020 Variation in albedo and its relationship with surface dust at Urumqi Glacier no. 1 in Tien Shan, China; *Front. Earth Sci.* **8** 110, <https://doi.org/10.3389/feart.2020.00110>.

Springer Nature or its licensor (e.g. a society or other partner) holds exclusive rights to this article under a publishing agreement with the author(s) or other rightsholder(s); author self-archiving of the accepted manuscript version of this article is solely governed by the terms of such publishing agreement and applicable law.